Theory and Application of an Analytical Approach for the Determination of the Transmission of Sound Waves through a Turbomachinery Stator

Peter Puttkammer [1], Maximilian Behn [2], Ulf Tapken [2],
Nicolas Thouault [3], Rob Hagmeijer [1]

[1] *University of Twente, Engineering Fluid Dynamics, Enschede, The Netherlands*

[2] *German Aerospace Center (DLR), Institute of Propulsion Technology, Engine Acoustics Department, Berlin, Germany*

[3] *MTU Aero Engines GmbH, Department Aerodynamics, Aeroelasticity, Aeroaucoustics Turbine, Munich, Germany*

The application of the two-dimensional aeroacoustic blade row model of Smith [1] to stators of axial turbomachines is investigated in detail. The study is part of an ongoing research project including the verification of the model by comparison with data from experiments and from CFD/CAA codes. The overall objective is the accurate prediction of the transmission and reflection of sound waves, which is of large interest with regard to the pre-design of turbomachinery blade rows.

The underlying concepts, related to the wave number, the phase velocity and the group velocity of the incoming 2D plane waves, are examined thoroughly. The 2D blade row model is applied to predict the sound transmission and reflection through a 3D stator and outcomes are compared with results of the CFD code Lin3D provided by MTU Aero Engines. For the approximation of the sound waves and the geometry using the 2D model parameters different approaches are developed and discussed. It is shown that the accuracy of the prediction can be improved by incorporating the effect of the impedance jump that corresponds to the change in cross-sectional area due to the stator blades.

Introduction

The analytical 2D aeroacoustic blade row model of Smith [1] is applied for predicting the transmission and reflection of sound waves through a turbomachinery stator. The underlying theory of the model is investigated thoroughly in [2], here the application of the model is presented.

Model description

In 2D, the annular blade row of the stator is represented by an unwrapped row of flat plates with zero thickness (annular strips), as displayed in Fig. 1. Such a cascade represents the 3D stator at a specific radius r from the centre of the of the circular duct, known as a radial strip. The blade row is infinitely long in y-direction with blade gap s between the blades, blade chord c and stagger angle α_s.

A sound wave attacking the blade row causes a non-zero normal velocity distribution on the blade surfaces. In order to satisfy the impermeability condition, a vorticity distribution over the blade surface is introduced. The model of Smith leads to a relation between the vorticity distribution and the magnitudes of the transmitted and reflected sound waves. This enables one to calculate the transmission and reflection coefficients, defined by:

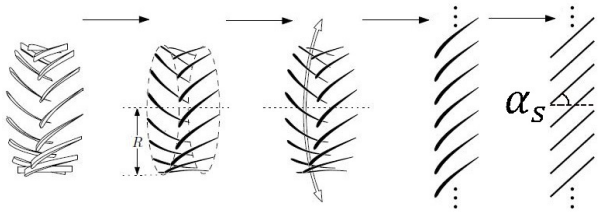

Figure 1: 2D cascade model representing a 3D stator. Figure from [3].

$$\mathcal{T} = \frac{|\bar{p}_t + \bar{p}_{inc}|}{|\bar{p}_{inc}|}, \quad \mathcal{R} = \frac{|\bar{p}_r|}{|\bar{p}_{inc}|}. \tag{1}$$

Here $\bar{p}_{inc}$, $\bar{p}_t$ and $\bar{p}_r$ are respectively the amplitudes of the incoming, transmitted and reflected sound waves.

Dispersion relation

Consider a 2D plane time-harmonic plane wave for pressure perturbations $p(\boldsymbol{x}, t)$:

$$p(\boldsymbol{x}, t) = \bar{p} e^{i(\boldsymbol{k}\cdot\boldsymbol{x} - \omega t)}, \tag{2}$$

where ω is the angular frequency and $\boldsymbol{k}$ is the wave number (with x- and y-components k_x and k_y), which is not equal to the free field wave number $k_{ff} = \omega/a$ due to the influence of the non-zero mainstream flow velocity. Substitution into the 2D convected wave equation (CWE) leads to the dispersion relation:

$$(\omega - \boldsymbol{U}\cdot\boldsymbol{k})^2 - (a|\boldsymbol{k}|)^2 = 0, \tag{3}$$

where $\boldsymbol{U}$ is the mainstream flow velocity and a is the speed of sound in air.

2D wave characteristics

For the interpretation of the latter results, a profound understanding of the phase velocity respectively the group velocity of the investigated sound wave is important.

Phase velocity

The phase velocity is the speed at which the phase of the wave propagates in space:

$$\boldsymbol{u}_\phi = a\hat{\boldsymbol{k}} + \left(\boldsymbol{U}\cdot\hat{\boldsymbol{k}}\right)\hat{\boldsymbol{k}}, \quad \hat{\boldsymbol{k}} = \frac{\boldsymbol{k}}{|\boldsymbol{k}|}, \tag{4}$$

such that the material derivative of the phase is zero:

$$\frac{\partial \phi}{\partial t} + \boldsymbol{u}_\phi \cdot \boldsymbol{\nabla}\phi = 0, \quad \phi = \boldsymbol{k} \cdot \boldsymbol{x} - \omega t. \tag{5}$$

Eq. 4 indicates that the phase velocity is only influenced by the mainstream flow velocity components normal to the wavefront (see Fig. 2). Interpreting the definition of the phase velocity (Eq. 4) and Fig. 2 demonstrates that the direction of the phase velocity determines the orientation of the wavefront.

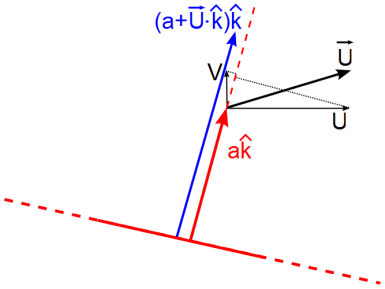

Figure 2: Phase velocity of plane sound waves. The red vector $a\hat{\boldsymbol{k}}$ is the velocity of the wave front in a quiescent medium. The black vector $\boldsymbol{U}$ is the velocity of the moving medium with x- and y-components U and V. The blue arrow represents the phase velocity vector.

Group velocity

The group velocity of a plane wave is defined as:

$$\boldsymbol{u}_g = \frac{\partial \omega(\boldsymbol{k})}{\partial \boldsymbol{k}} = a\hat{\boldsymbol{k}} + \boldsymbol{U}, \tag{6}$$

Where the dispersion relation (Eq. 3) has been used for $\omega(\boldsymbol{k})$. The group velocity is the the speed at which the energy of a wave is transported. The energy of the plane wave is proportional to:

$$E \sim E_0 e^{2i(\boldsymbol{k}\cdot\boldsymbol{x}-\omega t)}, \tag{7}$$

which shows that indeed:

$$\frac{\partial E}{\partial t} + \boldsymbol{u}_g \cdot \boldsymbol{\nabla} E = 0. \tag{8}$$

The wavefront does not only propagate in normal direction of the wavefront, it is transported by the velocity

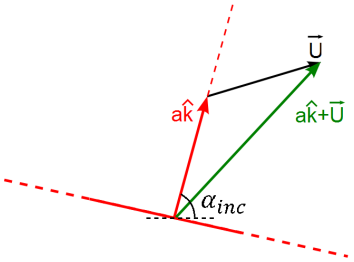

Figure 3: Group velocity of plane sound waves. The red vector $a\hat{\boldsymbol{k}}$ is the velocity of the wave front in a quiescent medium. The black vector $\boldsymbol{U}$ is the velocity of the moving medium. The green vector represents the group velocity vector.

of the sound wave and the convection velocity of the fluid (see Fig. 3).

Especially the axial component of the group velocity is an important quantity when analysing the blade row model. The direction of the group velocity determines the propagation direction of the plane wave. Downstream propagating waves are characterized by positive group velocities. Notice that the group velocity can be positive, whereas the phase velocity can be smaller then zero.

Results for 2D stator

Applying the implemented blade row model of Smith yields the satisfying result presented in Fig. 4, where three interesting conditions can be distinguished (arrows 1, 2 and 3).

When the wavefront is orientated normal to flat blades, total transmission occurs (arrow 1 in Fig. 4). The wave does not experience the presence of the infinitely thin flat plates (Fig. 5). This condition is known as the Venetian Blind condition [4].

A related, but much less intuitive, condition (modal condition [4], arrow 2 in Fig. 4) is the situation when the reflected waves are perpendicular to the blades (Fig. 6). These reflected waves cannot be induced by the singularity distribution over the flat plates.

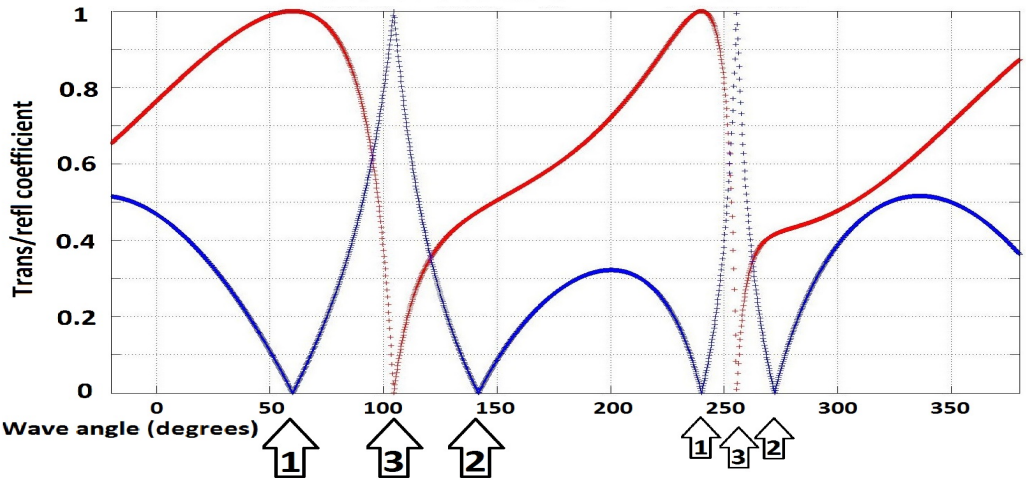

Figure 4: Transmission (red) $\mathcal{T}$ and Reflection (blue) $\mathcal{R}$ coefficients (Eq. 1) for incoming upstream (between 105° and 255°) and downstream (between 0° and 105° *and* 255° and 360°) propagating sound waves. Input parameters: $M = 0.5$, $s/c = 1$, $\alpha_s = 60°$ and $f = 850$Hz.

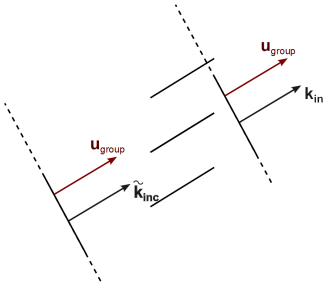

Figure 5: Venetian Blind condition: total transmission, zero reflection. $\alpha_{inc} = 60°$.

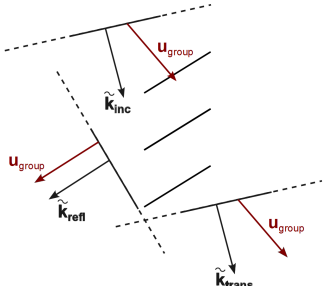

Figure 6: Modal condition: Zero reflection, however not total transmission. $\alpha_{inc} = 272°$.

The third condition is related to cases of total reflection (arrow 3 in Fig. 4). This occurs when the axial group velocity of the incoming wave is zero, hence no transportation of energy in axial direction (Fig. 7). Notice that this is not similar to wavefronts parallel to the flat plates (broadside condition in [4]). Here this condition is labelled the blocking condition, referring to the total reflection of sound waves.

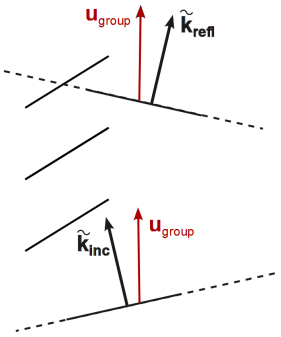

Figure 7: Blocking condition: Zero transmission, total reflection. $\alpha_{inc} = 105°$.

Results for 3D stator

The applicability of Smith's 2D model to real geometries is assessed by comparison with the results of 3D numerical calculations. These 3D reference results are obtained from the CFD code Lin3D, provided by MTU Aero Engines. Effort is made for appropriately representing 3D sound waves in terms of 2D parameters. Three different stagger angles for the 2D flat plates are used in order to investigate the accuracy of the 2D model. The sound waves in Lin3D are generated upstream of the stator by a constant pressure disturbance over the cross-sectional area of the duct with amplitude $\bar{p}$. The results are presented in terms of the sound power level (PWL) differences of the incoming and transmitted $\Delta\mathrm{PWL}_t$ and reflected waves $\Delta\mathrm{PWL}_r$, calculated using Tapken and Enghardt [5].

Test Case 1: 1 radial strip, pressure amplitude

Comparing the 2D (from Eq. 3) and 3D [6] wave numbers shows that these coincide precisely under the unique condition that:

$$R^* = \frac{m}{\sigma_{mn}} R_o. \tag{9}$$

Here m is the circumferential mode order, σ_{mn} the mode eigenvalue and R_o the outer radius of the circular duct. This radius R^*, named by Chapman as the caustic radius [7], is applied for analysing the 3D stator as a 2D unwrapped blade row. As input amplitude the pressure amplitude is selected, as visualized in Fig. 8.

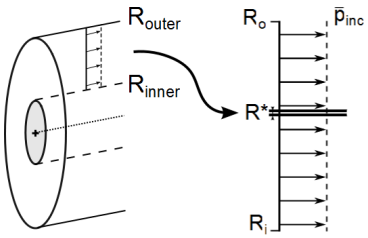

Figure 8: Schematic representation of test case 1.

Test Case 2: 5 annular section, mode amplitude

Analysing the cut-on factor (see [5]) for applied input parameters shows that only the radial mode orders $n = 0$ and $n = 1$ (for circumferential mode orders $m = -12..12$) are cut-on. The incoming mode amplitudes can be calculated using a so-called pseudo-inverse of the matrix filled with modal shape factors $[f]^*$ [6]:

$$\underline{A}_{inc} = [f]^* \underline{p}_{inc}. \tag{10}$$

Applying these mode amplitudes at 5 different radii, as visualized in figure 9, yields two matrices with respectively the transmission $[t]$ and reflection $[r]$ coefficients for every radial mode order and every radius as elements.

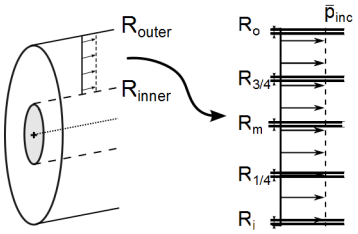

Figure 9: Schematic representation of test case 2.

The transmitted wave amplitude (reflected wave goes analogous) can be written similar as Eq. 10 as:

$$\underline{p}_t = [f]\underline{A}_t. \tag{11}$$

However the transmitted pressure wave amplitude can also be written using the transmission matrix:

$$\underline{p}_t = \big([f] \circ [t]\big)\underline{A}_{inc}. \tag{12}$$

Where $\circ$ indicates the Hadamard product. Applying Eq. 11 and 12 shows that the transmitted (and reflected) mode amplitudes can be calculated by applying:

$$\underline{A}_t = [f]^*\big([f] \circ [t]\big)\underline{A}_{inc}. \tag{13}$$

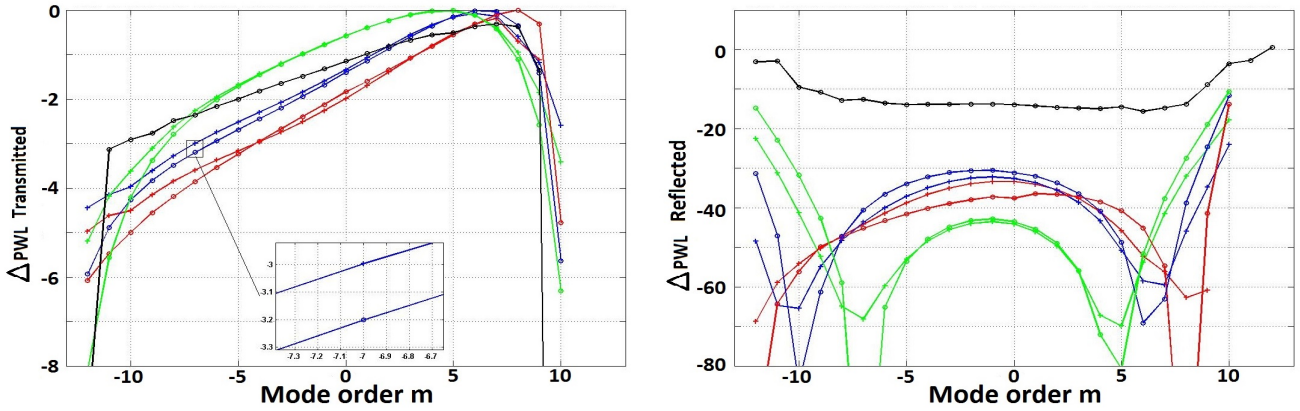

Figure 10: Differences of the sound power of the transmitted (left) and reflected (right) waves for test cases 1 (o) and 2 (+). Three different stagger angles: $\alpha_s = 55°$ (red), $\alpha_s = 42°$ (blue) and $\alpha_s = 29°$ (green). The black graph corresponds to the result of Lin3D.

The transmitted and reflected mode amplitudes (for $n = 0$ and $n = 1$) are consequently used in order to calculate the ΔPWL of the transmitted and reflected waves.

Results

The results of test cases 1 and 2 are presented in Fig. 10. Analysis shows that the transmission of 3D sound waves can be predicted to a reasonable extend, however the reflection is underestimated significantly by the model of Smith. It can be argued that test case 2 represents the reference results of Lin3D more accurate. The underestimation of the reflection can be caused by the infinitely flat plates applied in the model. Taking into account the impedance jump due to the changing cross-sectional area (duct with and without stator) yields a rough estimation of the reflection: $\Delta\text{PWL}_r = -17.1$. The relatively constant reflection curve can be explained rather accurately using the reflection coefficient based on the jump in cross-sectional area.

Conclusion and Outlook

The application of the 2D blade row model of Smith [1] in order to predict the transmission and reflection of sound waves through a turbomachinery stator is investigated. Comparison with the results of the original paper of Smith shows perfect agreement. Furthermore interesting conditions such as the Venetian Blind condition, the modal condition and the blocking condition are pointed out. Comparison with the results of Lin3D, incorporating the effect of the impedance jump due to the changing cross-sectional area, shows that the transmission and reflection of 3D sound waves can be predicted reasonably accurate.

The present study is part of an ongoing research project of DLR. In the near future experiments are planned in order to examine the applicability of the model of Smith even more.

References

[1] S. Smith. Discrete frequency sound generation in axial flow turbomachines. *Aeronautical Research Council Reports and Memoranda*, 1972.

[2] P. Puttkammer. Theory and Application of an Analytical Approach for the Determination of the Transmission of Sound Waves through a Stator. Msc. Report, *University of Twente & Engine Acoustics Dept. DLR*, 2015.

[3] G. Jenkins. Models for the prediction of rear-arc and forward-arc fan broadband noise in turbofan engines. PhD thesis, *University of Southampton*, 2013.

[4] D. B. Hanson. Acoustic reflection and transmission of 2-dimensional rotors and stators, including mode and frequency scattering effects. *AIAA Paper*, 1999.

[5] U. Tapken and L. Enghardt. Optimisation of sensor arrays for radial mode analysis in flow ducts. *AIAA paper*, (2006-2638), 2006.

[6] U. Tapken, T. Raitor, and L. Enghardt. Tonal noise radiation from an uhbr fanoptimized in-duct radial mode analysis. *Proceedings of the 15th AIAA/CEAS Aeroacoustics Conference, Miami, FL, May*, pages 11-13, 2009.

[7] C. Chapman. Sound radiation from a cylindrical duct. part 1. ray structure of the duct modes and of the external field. *Journal of Fluid Mechanics*, 281:293-311, 1994.